



Deposited via The University of Leeds.

White Rose Research Online URL for this paper:

<https://eprints.whiterose.ac.uk/id/eprint/161872/>

Version: Accepted Version

Article:

Monge-Morera, M, Lambrecht, MA, Deleu, LJ et al. (2020) Processing Induced Changes in Food Proteins: Amyloid Formation during Boiling of Hen Egg White. *Biomacromolecules*, 21 (6). pp. 2218-2228. ISSN: 1525-7797

<https://doi.org/10.1021/acs.biomac.0c00186>

This document is the Accepted Manuscript version of a Published Work that appeared in final form in *Biomacromolecules*, copyright © American Chemical Society after peer review and technical editing by the publisher. To access the final edited and published work see <https://doi.org/10.1021/acs.biomac.0c00186>.

Reuse

Items deposited in White Rose Research Online are protected by copyright, with all rights reserved unless indicated otherwise. They may be downloaded and/or printed for private study, or other acts as permitted by national copyright laws. The publisher or other rights holders may allow further reproduction and re-use of the full text version. This is indicated by the licence information on the White Rose Research Online record for the item.

Takedown

If you consider content in White Rose Research Online to be in breach of UK law, please notify us by emailing eprints@whiterose.ac.uk including the URL of the record and the reason for the withdrawal request.

This is the final draft post-refereeing.

The publisher's version can be found at <https://pubs.acs.org/doi/10.1021/acs.biomac.0c00186>

Please cite this article as: Monge-Morera, M. Lambrecht, M.A., Deleu, L.J., Gallardo, R., Louros, N.N., De Vleeschouwer, M., Rousseau, F., Schymkowitz, J. and Delcour, J.A.

Processing induced changes in food proteins: amyloid formation during boiling of hen egg white, *Biomacromolecules*, 2020, xx, xxxx-xxxx, doi: xxxxxx.

1 Processing induced changes in food proteins: 2 amyloid formation during boiling of hen egg white

3
4 *Margarita Monge-Morera¹, Marlies A. Lambrecht¹, Lomme J. Deleu¹, Rodrigo Gallardo^{2,3},*
5 *Nikolaos N. Louros², Matthias De Vleeschouwer², Frederic Rousseau^{2*}, Joost Schymkowitz^{2*},*
6 *Jan A. Delcour^{1*}*

7 ¹KU Leuven, Laboratory of Food Chemistry and Biochemistry and Leuven Food Science and
8 Nutrition Research Centre (LFoRCe), Kasteelpark Arenberg 20, B-3001 Leuven, Belgium

9 ²KU Leuven, Switch laboratory, Department of Cellular and Molecular Medicine, Herestraat 49,
10 B-3001 Leuven, Belgium

11 ³University of Leeds, Astbury Centre for Structural Molecular Biology, School of Molecular and
12 Cellular Biology, Garstang Building, LS2 9JT Leeds, United Kingdom

13 *Corresponding authors: frederic.rousseau@kuleuven.vib.be (Tel: +3216372572),
14 joost.schymkowitz@kuleuven.vib.be (Tel: +3216372573), jan.delcour@kuleuven.be (Tel:
15 +3216321581)

16 ABSTRACT

17 Amyloid fibrils (AFs) are highly ordered protein nanofibers composed of cross β -structure that
18 occur in nature, but that also accumulate in age-related diseases. Amyloid propensity is a generic
19 property of proteins revealed by conditions that destabilise the native state, suggesting that food
20 processing conditions may promote AF formation. This had only been shown for foie gras, but not
21 in common foodstuffs. We here extracted a dense network of fibrillar proteins from commonly
22 consumed boiled hen egg white (EW), using chemical and/or enzymatic treatments. Conversion
23 of EW proteins into AFs during boiling was demonstrated by thioflavin T fluorescence, Congo red
24 staining and X-ray fibre diffraction measurements. Our data show that cooking converts
25 approximately 1-3% of the protein in EW into AFs, suggesting that they are a common component
26 of the human diet.

27 KEYWORDS: cross β -sheet, food protein aggregation, ovalbumin, enzymatic or chemical
28 extraction, X-ray diffraction pattern

29

30

31

32

33 INTRODUCTION

34 Protein amyloid fibrils (AFs) are self-assembled fibrillar protein aggregates with a cross β -sheet
35 core. The β -strands are stacked perpendicular to the fibril axis and stabilised by hydrogen bonds^{1,2}.
36 This structure endows the fibrils with a remarkable chemical resistance and mechanical strength³,
37 making AFs interesting building blocks for functional protein-based materials^{4,5}. AFs occur in
38 nature, for instance, bacteria employ them as a colonization tool, insect larvae in their eggshells,
39 and even in mammals AFs are functionally employed, for example to regulate melanin
40 synthesis, hormone storage or memory formation^{6,7}. Moreover, AF formation is much studied in
41 the context of age-dependent degenerative conditions, including neuronal pathologies such as
42 Alzheimer or Parkinson's and non-neuronal diseases, such as type 2 diabetes or systemic
43 amyloidosis⁸. Despite the fact that only 40 or so amyloid-associated diseases are known,
44 bioinformatics work showed that amyloid propensity is widespread in the proteome and encoded
45 by aggregation prone polypeptide segments⁹⁻¹¹. The amyloid propensity is inhibited by the native
46 fold of the protein and can be revealed by exposing the protein to conditions that destabilise native
47 state, such as low pH or elevated temperature⁸. Common food-processing methods thus include
48 conditions that have been shown to promote amyloid formation for many proteins¹², including
49 food-borne proteins in purified form^{13,14}. However, prior to the present work, the only food in
50 which AFs have indisputably been shown to be present are duck and goose derived foie gras¹⁵.

51 Heating the commonly consumed hen (*Gallus gallus domesticus*) egg white (EW) induces
52 protein network and gel formation during which intermolecular β -sheet structures are formed^{5,16,17}.
53 Ovalbumin (OVA) (*ca.* 54%), ovotransferrin (*ca.* 12%), ovomucoid (*ca.* 11%), ovomucin (*ca.* 4%)
54 and lysozyme (*ca.* 4%) are the most abundant EW proteins¹⁸. AF formation is studied with isolated
55 OVA, lysozyme and EW as a whole¹³. Desalted solutions of EW powder (73 g/L) form short linear

56 aggregates of about 20 to 150 nm as a result of heating (78 °C for 22 h at pH 7.0), cooling (to
57 20°C) and adjusting the pH to 4.5. Their contour length is longer (50-350 nm rather than 20-150
58 nm) when EW preparations do not contain ovotransferrin¹⁹. Stretched films of poached EW show
59 X-ray diffraction patterns compatible with cross- β structures²⁰. Yet, the level of EW amyloid-like
60 aggregates is lower than obtained with solutions of pure OVA⁵. When heated to between 65 °C to
61 90 °C at acidic pH²¹⁻²⁶ or to between 40 °C to 80 °C at neutral pH for several hours to days^{5,23,27-}
62 ³³ OVA forms amyloid-like protein fibrils. The impact of processing on AF formation from OVA
63 was recently reviewed¹³. Heat-treated OVA [2.0% (w/v), pH 2.0 or 7.0, 60 °C to 80 °C, 60 or 1200
64 min] amyloid-like aggregates consist of a compact core surrounded by loosely packed protein
65 segments^{23,29}. Semi-flexible unbranched fibrils with contour lengths of 400 to 700 nm result from
66 heating 2.0% (w/v) OVA at 78 °C for 22 h at neutral pH and low ionic strength²⁷. However, the
67 typical X-ray diffraction pattern of the cross- β motif has not been described for heated OVA
68 amyloid-like aggregates. In spite of the above work, the potential presence of fibrils in boiled eggs
69 which meet all criteria to be classified as AFs remained to be investigated.

70 **We here show that AFs are formed during egg boiling.** That EW rapidly gels upon boiling
71 evidently complicates the identification of fibrillary protein structures as most methods require
72 protein to be solubilised/suspended. To overcome this problem, fibrillary structures were extracted
73 from EW gels using chemicals or enzymes. Compact amyloid structures are less susceptible to
74 chemical or enzymatic cleavage than amorphous protein aggregates^{14,34-36}. We successfully used
75 proteinase K and subsequent solubilisation with hydrochloric acid solution to extract fibrils from
76 boiled EW. These fibrils were indisputably identified as AFs.

77

78

79

80 EXPERIMENTAL SECTION

81 **Materials.** EW [*ca.* 90% protein on dry matter (dm) basis] was isolated from commercial eggs
82 as commonly done. Dithiothreitol and sodium azide were from Acros Organic (Geel, Belgium).
83 Sodium dodecyl sulfate, sodium dihydrogen phosphate dihydrate, sodium chloride and urea were
84 from VWR International (Leuven, Belgium). Bovine serum albumin standard (23209) was from
85 ThermoFisher Scientific (Waltham, MA, USA). OVA (albumin chicken egg grade III, *ca.* 94%
86 protein on dm basis), proteinase K (*Tritirachium album*, P4850), trypsin (porcine pancreas, T0303)
87 and all chemicals (of at least analytical grade), unless specified otherwise, were from Sigma
88 Aldrich (Bornem, Belgium). Enzyme units (EU) were as specified by the supplier. The highly
89 amylogenic peptide (residues: 103-111) derived from sup35 yeast was produced in-house³⁷.

90 **Heat treatment of egg white and ovalbumin.** Fresh EW (15.0 g) was boiled for 15 min at
91 100 °C in sealed plastic cans (inner and outer diameters 4.0 cm and 4.3 cm respectively, height =
92 3.0 cm). The core of the EW gel was cut in small pieces and used in further analysis. An aliquot
93 (1.0 ml) of 5.0% (w/v) OVA was heated in sealed glass tubes (inner and outer diameters 1.2 and
94 1.5 cm respectively, height = 10 cm) at 78 °C and 100 °C for different times. Also, 2.0 ml 2.0%
95 (w/v) OVA was heated at 78 °C for 22 h (OVA_{78/22h}) as described previously²⁷.

96 **Protein fibril isolation.** To unheated and heated samples containing about 32.0 mg of OVA or
97 EW protein was added an amount of SDS and/or DTT containing medium such that a total volume
98 of 1.6 ml was obtained which contained 0.0%, 0.1%, 0.2%, 0.3%, 0.5% or 0.8% (w/v) SDS, 0.02%
99 (w/v) sodium azide and, optionally, 1.0% (w/v) DTT. The samples were shaken at room
100 temperature (RT) (16 h, 150 rpm). The supernatants obtained by centrifugation (9,300 g, 15 min,
101 RT) were analysed.

102 **Enzymatic treatment and protein fibril isolation.** Aliquots of proteinase K (5.2 μ l containing
103 *ca.* 4 EU) or trypsin (13 μ l containing *ca.* 3.38 to 5.20 kEU) were added to samples containing *ca.*
104 32.0 mg (un)heated protein. The samples were then incubated at 37 °C for 48 h under continuous
105 shaking (150 rpm). The supernatant (*i.e.* soluble fraction 1) obtained by centrifugation (9,300 g,
106 15 min, RT) was analysed. Protein fibrils contained in the separated EW pellet produced after
107 proteinase K treatment (*ca.* 75.0 mg) were extracted (RT, 1 h, 150 rpm) by adding aliquots (1.5
108 ml) of 0.01 M, 0.05 M, or 0.1 M HCl. The supernatants (*i.e.* soluble fraction 2) obtained by
109 centrifugation (9,300 g, 15 min, RT) were analysed.

110 **Analysis of protein content.** The protein contents of diluted OVA and EW extracts obtained
111 after chemical or enzymatic treatment were determined in triplicate by analysis of ultraviolet (UV)
112 extinction (280 nm). Samples (200 μ l) transferred to UV-star plates (Greiner Bio-One, Vilvoorde,
113 Belgium) were analysed in a Synergy Multi-Mode Microplate Reader (BioTek, Winooski, VT,
114 USA). Absorbance values were converted to protein concentrations using a calibration curves
115 constructed with unheated OVA and EW ($R^2= 0.9987$ and $R^2= 0.9974$; respectively).

116 **Analysis of thioflavin T fluorescence.** Thioflavin T fluorescence is an indication of the level
117 of cross- β sheet structures³⁸. In a black 96-well plate (Greiner Bio-One), sample (190 μ l) was
118 mixed with 10 μ l 200 μ M ThT. Triplicate fluorescence measurements were performed in a
119 Synergy Multi-Mode Microplate Reader (BioTek). The excitation and emission wavelengths were
120 440 nm and 480 nm, respectively. The reference [*i.e.* 2.0% (w/v) OVA_{78/22h}] and extracted/isolated
121 protein samples were diluted to the same protein content [0.05 % (w/v) or 0.1% (w/v)] with 0.05 M
122 sodium phosphate buffer (pH 7.0, SPB). This dilution with SPB buffer prevents differences in ThT
123 intensity due to differences in pH or viscosity. The latter can restrict the rotation of the
124 benzothiazole and the aminobenzene rings of the ThT molecule^{39,40}. ThT fluorescence is

125 expressed as the fluorescence intensity of the sample relative to that of the above mentioned sup35
126 yeast peptide (*i.e.* NFNYNLQG) under the applied experimental conditions.

127 **Microscopy of Congo red stained samples.** AFs have a typical green birefringence when
128 stained with Congo red. Enzyme treated OVA and EW protein samples were concentrated by
129 centrifugation (10,000 g for 15 min) using an Amicon Ultra-0.5 centrifugal filter device 50 K
130 (Merck, Darmstadt, Germany). Aliquots (first 10 μ l and 4 to 7 μ l for the subsequent additions) of
131 the concentrated samples were dried on a microscope slide repeatedly. After drying, 7 to 10 μ l
132 0.1% (w/v) Congo red was added (RT, 30 min, dark room). Afterwards, samples were washed
133 several times with 90% (w/w) ethanol prior to being studied under bright and polarised light with
134 a SM2 800 optical microscope (Nikon, Tokyo, Japan) equipped with a camera and Nikon NIS-
135 Elements Viewer 4.20 software.

136 **Size exclusion chromatography.** The apparent molecular weight (MW) distribution of protein
137 aggregates was evaluated in triplicate using SE-HPLC⁴¹. Samples (1.0 ml) combined with 43 μ l
138 200 μ M ThT were filtered (Millex-HP, 0.45 μ m, polyethersulfone; Millipore, Carrigtwohill,
139 Ireland) and loaded on a Biosep-SEC-S3000 (size range 5-700 kDa, 25 μ l, 0.5 ml SPB/min) or
140 Biosep-SEC-S4000 (size range 15-1,500 kDa, 23 μ l, 1.0 ml SPB/min) (Phenomenex, Torrance,
141 CA, USA) column at 30 °C. SE-HPLC was conducted using a LC-20AT system (Shimadzu,
142 Kyoto, Japan) with automated injection, monitoring 280 nm UV extinction, and using 450 and 480
143 nm as excitation and emission wavelengths for ThT fluorescence detection.

144 **Multi-angle light scattering.** The MW of the protein aggregates was studied using multi-angle
145 light scattering (MALS) on a DAWN HELEOS MALS instrument from Wyatt Technology (Santa
146 Barbara, CA, USA) with an incident laser wavelength of 658 nm. The protein aggregates were
147 separated by SE-HPLC with an LC-10 Prominence system (Shimadzu) using conditions similar as

148 described above. Duplicate aliquots (25 μ L) of a solution containing 2.0 mg protein/ml were
149 injected at RT. The scattering intensities at different angles were collected, corrected for the
150 refractive indices of glass and solvent and normalised using bovine serum albumin. The value of
151 dn/dc (wherein n is the refractive index of the solution and c the solute concentration) was set to
152 0.185 ml/g and the scattering data (collected at an interval of 0.5 seconds) were then fitted
153 according to Zimm formulation, which relates the excess of incident light scattered to the
154 molecular structure⁴².

155 **Transmission electron microscopy.** The morphology of protein aggregates was studied with
156 TEM. Samples (10 μ l) were loaded for 3 min on glow discharged copper grids of 400-mesh which
157 were coated with formvar film (Agar Scientific, Stansted, United Kingdom). After sample
158 adsorption, the excess sample was drained with filter paper. Then, samples were washed with
159 MilliQ water and stained with 2.0% (w/v) uranyl acetate in MilliQ water for 45 s. Stained samples
160 were washed a second time with MilliQ water and drained with filter paper. The grids were dried
161 for 5 min at RT and examined using a JEM-1400 TEM (Jeol, Tokyo, Japan) instrument at 80 keV.

162 **Attenuated total reflection Fourier transform infrared spectroscopy.** The secondary
163 structure of samples (35 μ l) containing 0.1% (w/v) protein was investigated with attenuated total
164 reflection Fourier transform infrared spectroscopy (ATR-FTIR) in a Bruker (Karlsruhe, Germany)
165 Tensor 27 infrared spectrophotometer equipped with a Bio-ATR II accessory (Harrick Scientific
166 Products, Pleasantville, NY, USA). The instrument was continuously purged with dry air. Spectra
167 were recorded in the 850 to 4,000 cm^{-1} range at a resolution of 2 cm^{-1} by accumulating 256 data
168 acquisitions, corrected for atmospheric water vapor interference, baseline-subtracted, and vector
169 normalised in the Amide I area (1,600 to 1,700 cm^{-1}). Maximum peaks were assigned with peak
170 picking based on the second derivative, as implemented in Bruker OPUS software.

171 **X-ray diffraction measurements.** The crystalline structure along the fibre axis was studied with
172 X-ray diffraction. Protein extracts concentrated by centrifugation (10,000 g for 15 min) using an
173 Amicon Ultra-0.5 centrifugal filter device (50 K) were dried and the fibres formed between two
174 wax tipped capillary tubes were analysed. X-ray diffraction patterns were collected using a Rigaku
175 (Tokyo, Japan) copper rotating anode (RA-Micro7 HFM) operated at 40 kV and 30 mA and a
176 wavelength $\lambda = 1.54 \text{ \AA}$. The specimen-to-film distance was 275 mm and the exposure time 900 s.
177 Diffraction patterns were studied using Adxv software (Scripps Research, La Jolla, CA, USA) and
178 displayed with iMosFLM⁴³.

179 **Statistical analysis.** Significant differences ($\alpha < 0.05$) based on at least three individual
180 measurements were determined with a one-way ANOVA procedure using JMP® Pro 14.0.0 (SAS
181 Institute, Cary, NC, USA). Corresponding Tukey grouping coefficients are given.

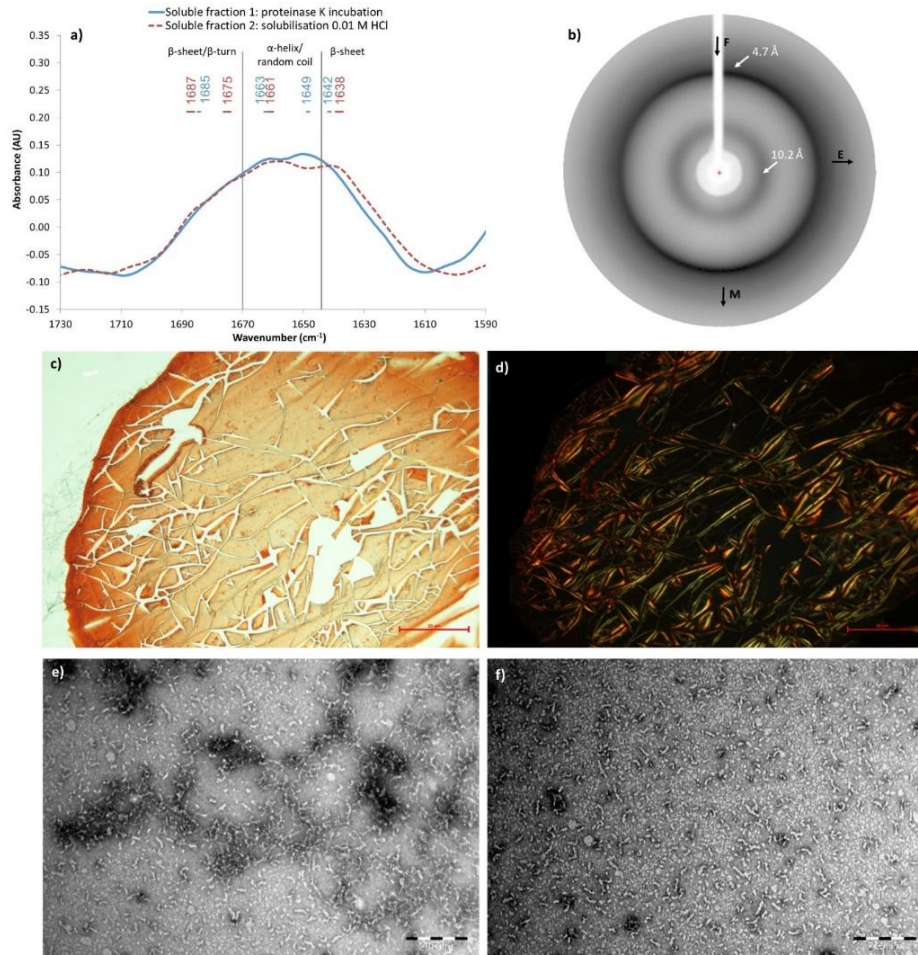
182

183 RESULTS AND DISCUSSION

184 **Identification of amyloid fibrils in boiled hen egg white**

185 AFs display the following properties that can hence be used to unequivocally identify this protein
186 structure: a fibrillar morphology as visualized by transmission electron microscopy (TEM), a high
187 level of β -sheet structures as shown by thioflavin T (ThT) fluorescence and Fourier transform
188 infrared (FTIR) spectroscopy, green birefringence upon staining with Congo red and, widely
189 regarded as the strongest evidence, a unique X-ray diffraction pattern with reflections at 4.7 \AA
190 (meridional) and $9\text{-}12 \text{ \AA}$ (equatorial), which correspond to the inter β -strand spacing and the
191 distance between stacked β -sheets, respectively^{2,44}. Dilute hydrochloric acid (HCl) (0.01 M, 0.05
192 M or 0.10 M) extracted almost all fibrillary EW structures in pellets obtained after proteinase K
193 treatment of 15 min boiled EW (EW_{100/15min}) resulting in ThT fluorescence values in the extracts

194 of *ca.* 20% compared with the intensity of a sample of mature AFs of yeast prion sup35 peptide
195 (residues: 103-111) at the same protein concentration in monomeric units. FTIR spectra of the 0.01
196 M HCl extract confirmed the presence of β -sheet structures (Figure 1.a). In addition, TEM images
197 indicated the presence of worm-like protein fibrils of variable sizes (Figure 1.e, Figure 1.f and
198 Figure S1). The extracted protein also showed the characteristic amyloid green birefringence after
199 staining with Congo red (Figure 1.c and Figure 1.d). Its X-ray diffraction pattern showed typical
200 amyloid reflections at 4.7 Å and 10.2 Å confirming that AFs are formed during EW boiling. An
201 estimated 1.5-3.0% of EW proteins assemble into AFs during boiling [calculated by comparing
202 the amount of protein of the size-exclusion high performance liquid chromatography (SE-HPLC)
203 peak A of the boiled EW tryptic digest with a high ThT fluorescence (Figure 3.e) and the initial
204 protein content].



205

206 Figure 1. Amyloid fibrils (AFs) in egg white (EW) boiled for 15 min ($EW_{100/15min}$). FTIR spectrum

207 (a) of soluble fraction 1 (proteinase K incubation of $EW_{100/15min}$) and of soluble fraction 2

208 (solubilisation with 0.01 M HCl of the pellet produced after proteinase K treatment of $EW_{100/15min}$).

209 Wavenumbers in (a) are detected with the peak picking tool based on the second derivative.

210 Vertical lines in (a) separate the wavenumbers assigned to the secondary structure of proteins. AU,

211 arbitrary units. X-ray diffraction pattern (b) of soluble fraction 2. Congo red stained sample of

212 pellet obtained from $EW_{100/15min}$ pellet after proteinase K treatment observed under bright light (c)

213 and under cross-polar light (d). Scale bar: 20 μm . Transmission electron microscopy (TEM)

214 images (e and f; scale bar: 200 nm) of the soluble fraction 2.

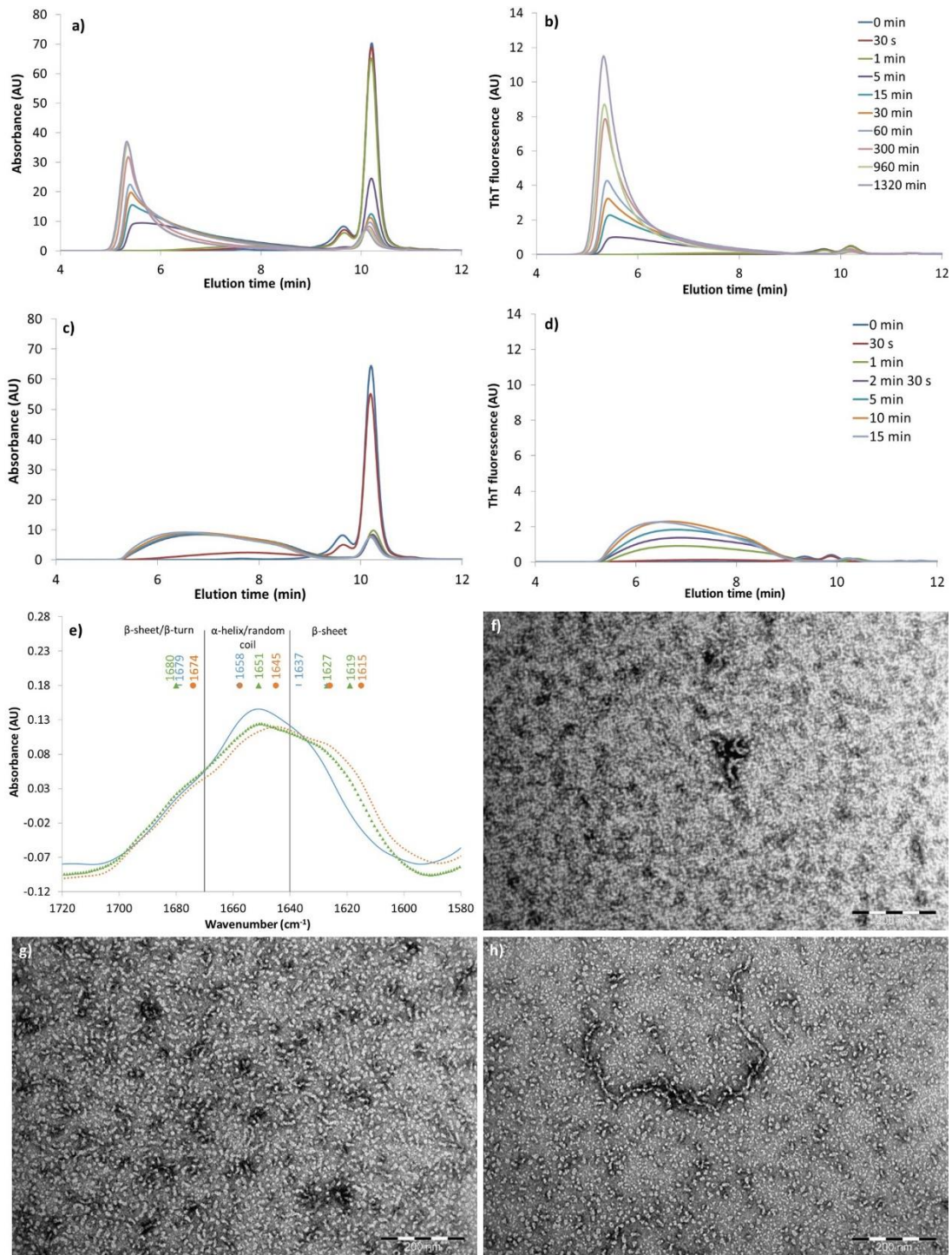
215

216 **Enzymatic digestion for isolating protein fibrils**

217 To exclude the impact of the extraction procedure on the formation of EW AFs, we tested the
218 above described proteinase K treatment also on OVA fibrils. OVA heated at 78 °C for 22 h
219 (OVA_{78/22h}) was included as positive control as it contained larger worm-like fibrils (Figure 2.a)
220 than OVA boiled for 15 min (OVA_{100/15min}) (Figure 2.c). Indeed, while TEM images of
221 OVA_{100/15min} (Figure 2.h and Figure S2) showed (clusters of) short worm-like fibrils with an
222 average length of maximally *ca.* 80 nm, OVA_{78/22h} (Figure 2.g and Figure S2) showed
223 predominantly short (< *ca.* 120 nm) but also longer (> *ca.* 200 nm) worm-like fibrillary protein
224 complexes. In addition, fluorescence density, *i.e.* the area of ThT fluorescence relative to that of
225 UV absorbance, measurements showed higher levels of β -sheet structures in OVA_{78/22h} than in
226 OVA_{100/15min}. In both samples, the maximum wavenumbers of the second derivative in the FTIR
227 spectrum indicated the presence of β -sheet structures (Figure 2.e). Noteworthy, non-aggregated
228 proteins and some large worm-like protein aggregates with a length of *ca.* 200 nm were detected
229 with TEM in native OVA (Figure 2.f and Figure S2).

230

231

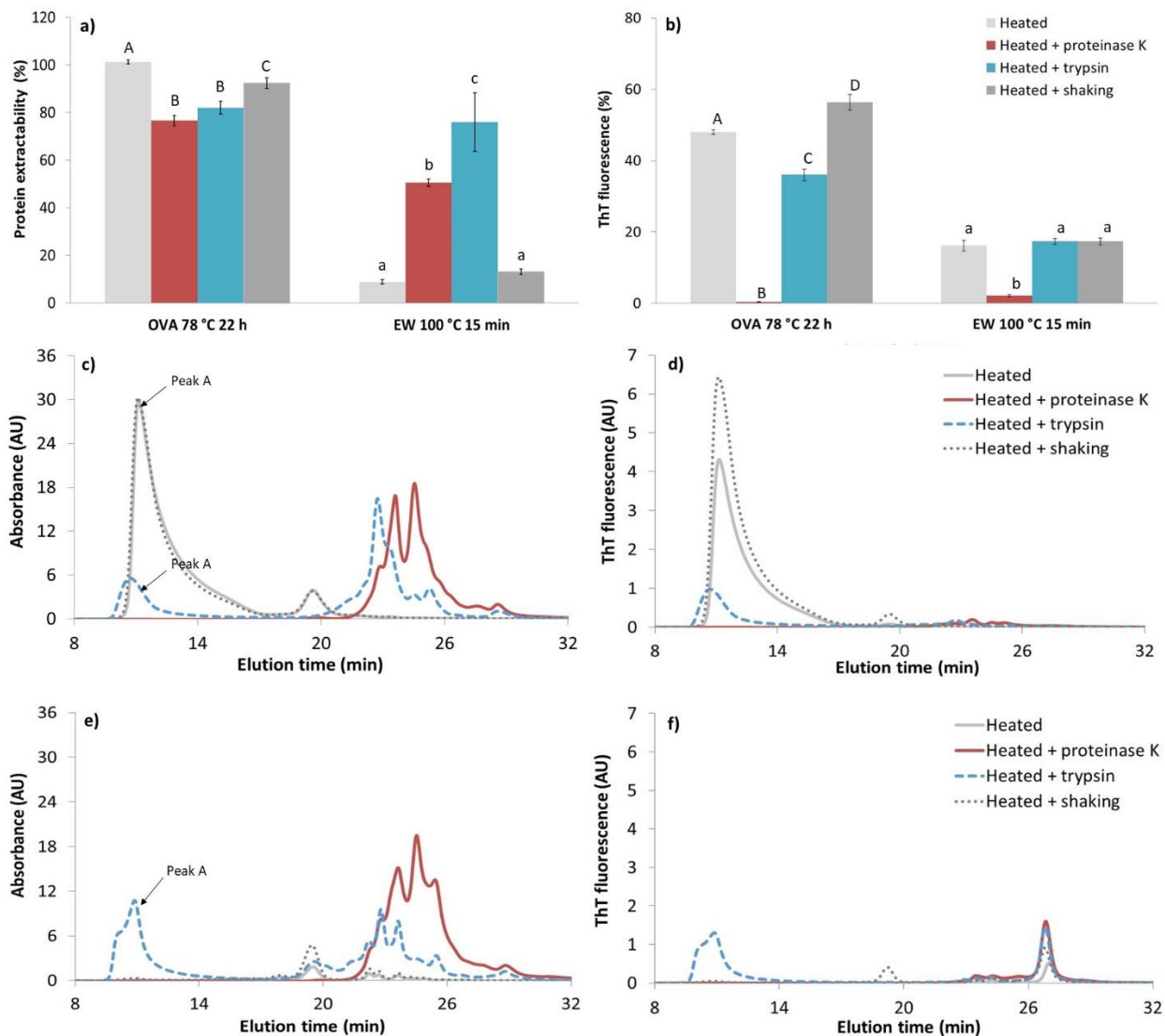


232

233 Figure 2. Impact of heating on ovalbumin (OVA) protein fibrillation. SE-HPLC profiles of
 234 ovalbumin (OVA) heated at 78 °C (a, b, OVA78) and 100 °C (c, d, OVA100) for various times.
 235 OVA showed peaks at ca. 9 min and 55 s and 10 min and 22 s which correspond to OVA dimers

236 (*ca.* 76 kDa) and monomers (*ca.* 40 kDa), respectively. UV absorbance (a, c) and thioflavin T
237 (ThT) fluorescence (b, d) were measured. FTIR spectrum (e) and transmission electron microscopy
238 (TEM) images (scale bar: 200 nm) of unheated (— in e, f) and heated ovalbumin (OVA) for 22 h
239 at 78 °C (..... in e, g, OVA_{78/22h}) and OVA heated for 15 min at 100 °C (▲ in e, h, OVA_{100/15min}).
240 Wavenumbers shown in (e) were detected with the peak picking tool based on the second
241 derivative. Vertical lines in (e) separate the wavenumbers assigned to the secondary structure of
242 proteins. AU, arbitrary units.

243 The supernatants obtained after 6 and 48 h proteinase K treatments of OVA_{78/22h} and EW_{100/15min}
244 and centrifugation (Figure 3.a and Figure S3) had ThT fluorescence readings which were
245 drastically lower than those of control samples which had undergone the same treatments but
246 without proteinase K addition (Figure 3.b and Figure S3). More in particular, SE-HPLC profiles
247 of OVA_{78/22h} and EW_{100/15min} extracts revealed no or only a slight enhancement in ThT fluorescence
248 as a result of proteinase K treatment (Figure 3.c and Figure 3.d, Figure 3.e and Figure 3.f,
249 respectively). In addition, TEM images of OVA_{78/22h} and EW_{100/15min} extracts obtained with 6 h
250 proteinase K treatment showed mainly amorphous protein aggregates (Figure 4 and Figure S4).
251 The above allowed speculating that the pellet recovered by centrifugation following proteinase K
252 treatment of OVA_{78/22h} and EW_{100/15min} contained AFs.

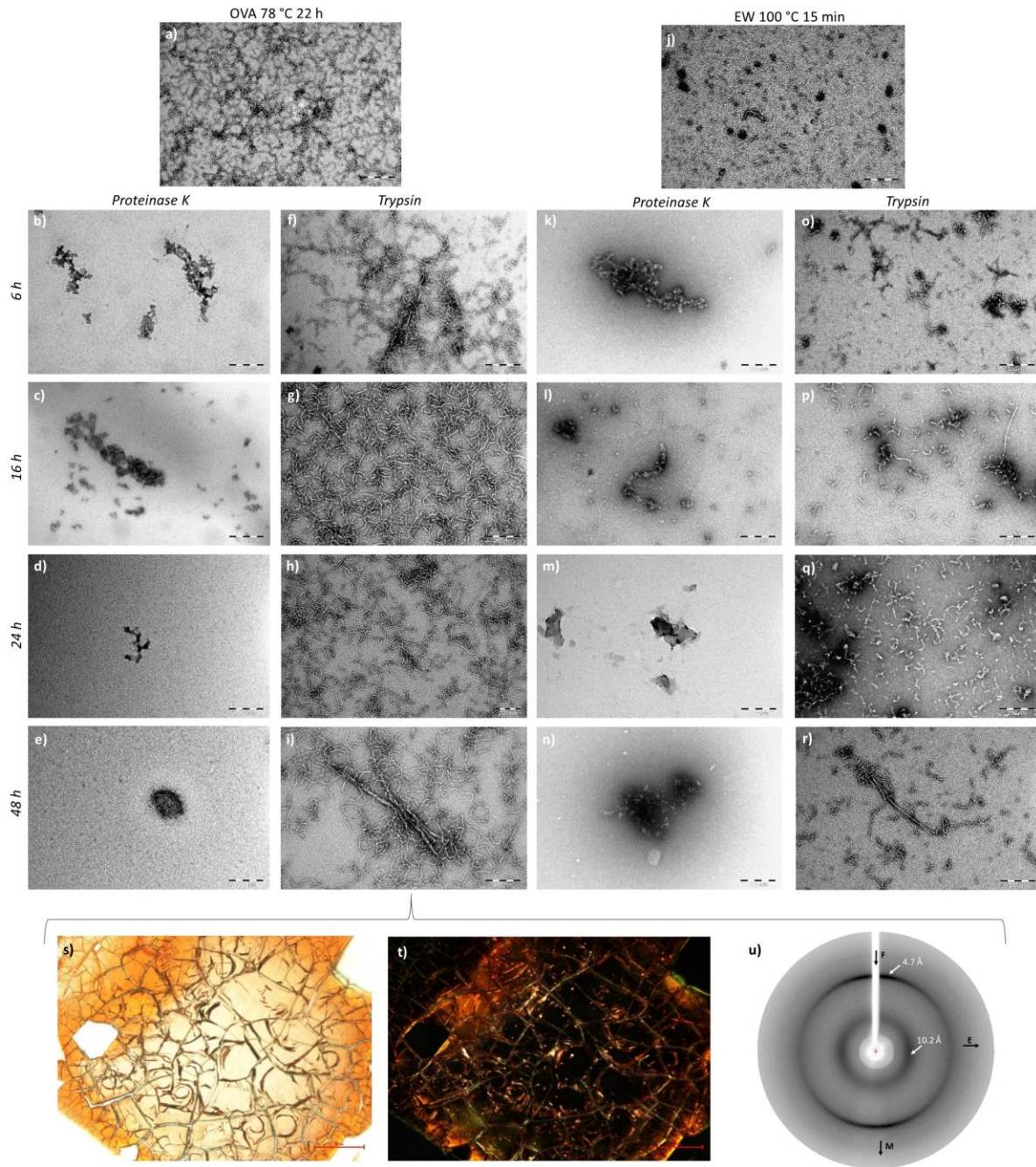


253

254 Figure 3. Impact of peptidase treatment on protein fibril extractability derived from heated
 255 ovalbumin (OVA_{78/22h}) and egg white boiled for 15 min (EW_{100/15min}). Protein extractability (a)
 256 and thioflavin T (ThT) fluorescence (b) of OVA_{78/22h} and EW_{100/15min} treated with proteinase K or
 257 trypsin. Shaking (150 rpm) was for 48 hours at 37 °C. Results with the same letters are not
 258 significantly different in OVA_{78/22h} (uppercase) and EW_{100/15min} (lowercase) [$P < 0.05$]. SE-HPLC
 259 UV profiles of OVA_{78/22h} (c, d) and EW_{100/15min} (e, f) treated with proteinase K or trypsin. UV
 260 absorbance (c, e) and thioflavin T (ThT) fluorescence (d, f) were measured. AU, arbitrary units.

261 In addition, an alternative method based on proteolytic degradation of the sample with trypsin
262 was developed. As trypsin preferentially cleaves after lysine and arginine residues and these
263 charged amino acids are generally not present in aggregation prone sequences leading to AFs, it
264 was also used in the present work to treat EW_{100/15min} or solutions of OVA_{78/22h}. When shaking
265 OVA_{78/22h} and EW_{100/15min} samples with trypsin, the isolation yield/extractability of protein from
266 both samples was about 80% (Figure 3.a). The ThT fluorescence of these samples was significantly
267 lower (for OVA_{78/22h}) or similar (for EW_{100/15min}) to that of those which also had been shaken, but
268 without enzyme (Figure 3.b). Trypsin treatment (6 h) caused a slight decrease in the ThT
269 fluorescence of the OVA_{78/22h} extract to a plateau value of *ca.* 36% (Figure S3). In contrast, the
270 ThT fluorescence of EW_{100/15min} (*ca.* 20%) was not impacted by the enzymatic treatment (Figure
271 S3). SE-HPLC profiles of OVA_{78/22h} and EW_{100/15min} samples treated with trypsin showed large
272 protein (peak A) aggregates (elution time *ca.* 10 – 12 min; *ca.* 15,000 k and 24,000 k respectively)
273 with enhanced ThT fluorescence (Figure 3.c and Figure 3.d, Figure 3.e and Figure 3.f,
274 respectively). In addition, large (> 200 nm) worm-like fibrillary aggregates were observed when
275 peak A material of OVA_{78/22h} and EW_{100/15min} was subjected to TEM (Figure S5). Mainly worm-
276 like fibrillary structures in combination with long (> 200 nm) straight protein fibrils were observed
277 after OVA_{78/22h} and EW_{100/15min} tryptic treatment (Figure 4 and Figure S4). In addition, the extract
278 obtained after OVA_{78/22h} tryptic treatment had characteristic amyloid green birefringence (Figure
279 4.s and Figure 4.f). Also, X-ray diffraction (Figure 4.u) showed meridional (4.7 Å) and equatorial
280 (10.2 Å) reflections typical of intra-β-strand and inter-β-sheet distances of AFs, respectively.
281 These results suggest that trypsin solubilised AFs from OVA_{78/22h}.

282



283

284 Figure 4. Characterisation of protein fibrils extracted with proteinase K and trypsin from heated
 285 ovalbumin (OVA_{78/22h}) and egg white boiled for 15 min (EW_{100/15min}). TEM images OVA_{78/22h} [(a)
 286 to (i)] and EW_{100/15min} [(j) to (r)] treated with proteinase K and trypsin over time. Scale bar: 200

287 nm. Congo red staining observed under bright (s) and cross-polar light (f) [Scale bar: 20 μ m] and
288 X-ray diffraction pattern (u) of OVA_{78/22h} treated with trypsin.

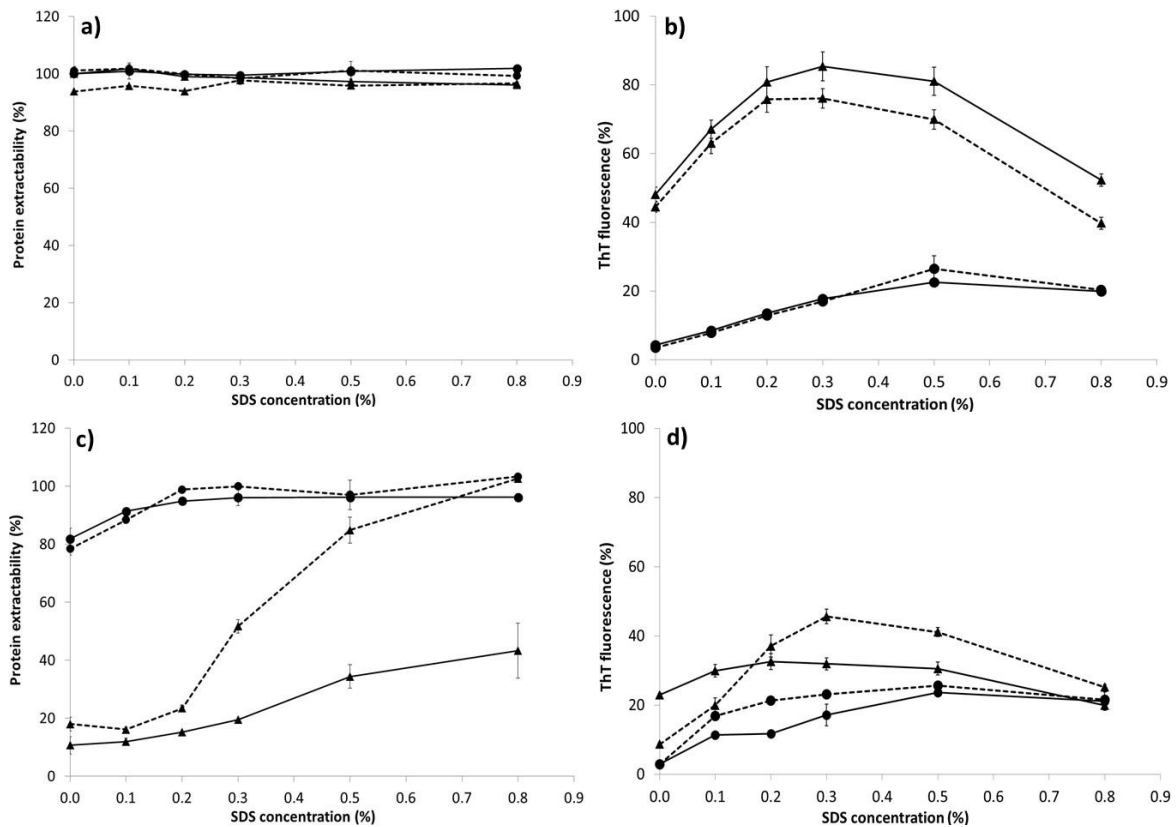
289 As a control treatment, OVA_{78/22h} was shaken in water for two days at 37 °C which resulted in
290 decreased protein extractability (Figure 3.a) and increased ThT fluorescence (Figure 3.b). Also,
291 the SE-HPLC profiles of OVA_{78/22h} showed protein aggregates [elution time 9 – 12 min; molecular
292 weight (MW) *ca.* 2,500 k; peak A] with higher ThT fluorescence when the samples had undergone
293 this shaking treatment (Figure 3.c and Figure 3.d). In addition, long (> 200 nm) worm-like
294 fibrillary aggregates were observed in peak A of shaken OVA_{78/22h} samples (Figure S5). The
295 observed increase in the level of fibrillary structures initially formed after heating OVA at 78 °C
296 during further shaking at 37 °C (150 rpm, two days) is in line with earlier reports that mechanical
297 agitation impacts the aggregation rate, size and morphology of protein fibrils^{45,46}. When unheated
298 OVA was shaken in water for two days at 37 °C protein aggregation also occurred but the ThT
299 fluorescence remained low (data not shown). EW_{100/15min} extracts contained about 10% protein
300 (Figure 3.a) with apparent MWs < 74 k (elution time \geq 18 min, Figure 3.e). Shaking of EW_{100/15min}
301 resulted in a negligible increase in the amount of peptides eluting between 17 and 18 min (MW
302 *ca.* 74 k) in the SE-HPLC profiles and some ThT fluorescence enhancement (Figure 3.e and Figure
303 3.f).

304 **Usage of chemicals for isolating protein fibrils**

305 As an alternative for enzymatic extraction, chemicals were used to extract AF from EW_{100/15min}.
306 Various concentrations of sodium dodecyl sulfate (SDS) and/or dithiothreitol (DTT) were used to
307 impact non-covalent interactions and/or disulfide bonds, respectively. While SDS binds to proteins
308 and modifies their secondary and tertiary structure^{47,48}, DTT reduces disulfide bridges in proteins
309 into thiol groups. Mainly worm-like fibrillary structures of variable sizes were observed for

310 EW_{100/15min} extracts in water and in 0.3% (w/v) SDS both in the presence (Figure S6) or absence
311 (Figure 6.j, Figure 6.k and Figure S6) of DTT. While all protein was extracted with 0.8% SDS
312 (w/v) containing DTT (Figure 5.c), such extraction resulted in lower (*ca.* 25%) ThT fluorescence
313 (Figure 5.d) than that with 0.3% SDS (w/v) containing DTT. TEM images (Figure 6.l and Figure
314 S6) of EW_{100/15min} in 0.8% (w/v) SDS showed protein fibrils. However, while the FTIR spectra of
315 EW_{100/15min} in 0.8% (w/v) SDS were characteristic for β -sheet structures, those in the same medium
316 also containing 1.0% (w/v) DTT were not (data not shown). With TEM, both amorphous
317 aggregates and protein fibrils were observed in the latter (Figure S6) The combined use of DTT
318 and the higher SDS concentrations for extracting protein from EW_{100/15min} resulted in disruption of
319 protein fibrils.

320 The same chemical extractions procedures were applied on OVA_{100/15min} samples as positive
321 control. While neither the protein extractability of unheated nor that of heated OVA were affected
322 by the concentrations of SDS and DTT used (Figure 5.a), the levels of ThT fluorescence were
323 (Figure 5.b). When using SDS concentrations in a 0.1% to 0.3% (w/v) range, the ThT fluorescence
324 of OVA_{100/15min} samples increased from *ca.* 48% to *ca.* 85% irrespective of whether the medium
325 contained 1.0% (w/v) DTT (Figure 5.a). SDS thus also induced fibril formation in OVA_{100/15min}
326 samples. However, the ThT fluorescence of OVA_{100/15min} samples was lower when the SDS levels
327 used exceeded 0.5% (w/v) both in the presence and absence of 1.0% (w/v) DTT (Figure 5.b). SDS
328 can thus also disrupt protein fibrils as also observed in unheated OVA samples at similar SDS
329 concentrations. In aqueous extracts of OVA_{100/15min}, mainly large (> 200 nm) intertwined worm-
330 like fibrillary aggregates were detected (Figure 6.d and Figure S6). At SDS concentrations of 0.3%
331 and 0.8% (w/v), the fibrils were *ca.* 100 nm (Figure 6.e and Figure S6) or *ca.* 40 nm (Figure 6.f
332 and Figure S6) long, respectively.



334

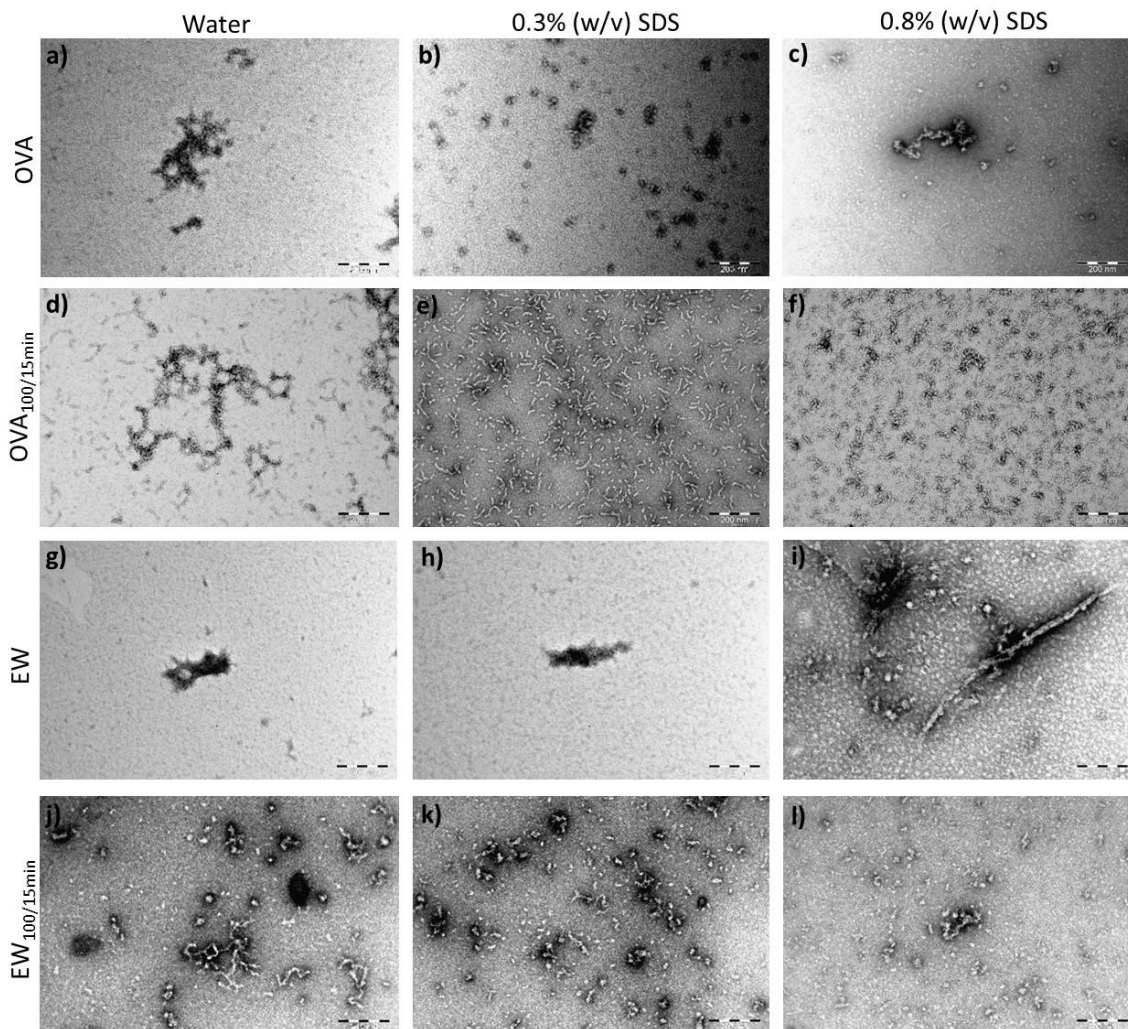
335 Figure 5. Impact of sodium dodecyl sulfate (SDS) and 1.0% (w/v) dithiothreitol (DTT) on protein
 336 fibril extractability from unheated ovalbumin (OVA) and egg white (EW) or boiled for 15 min
 337 OVA (OVA_{100/15min}) and EW (EW_{100/15min}). Protein extractability (a) and thioflavin T (ThT)
 338 fluorescence (b) of unheated OVA (a, b, ●) and EW (c, d, ●) or OVA_{100/15min} (a, b, ▲) and
 339 EW_{100/15min} (c, d, ▲) extracted with various concentrations of SDS without (—) and with 1.0%
 340 (w/v) DTT (---).

341 To exclude that the chemical extraction procedure itself influenced the amyloid content of the
 342 sample, the procedure was performed under native conditions. Dilution (5x) and shaking (150 rpm)
 343 of fresh EW induced aggregation and precipitation of *ca.* 20% of the protein. Its extractability and
 344 ThT fluorescence gradually increased with SDS concentrations in the extraction medium (Figure

345 5.c and Figure 5.d). More EW protein was extractable when the SDS medium also contained DTT
346 (Figure 5.c and Figure 5.d). Complete extractability was achieved with 0.8% (w/v) SDS
347 irrespective of whether the medium also contained DTT (Figure 5.c). Mostly amorphous
348 aggregates in combination with some large (> 200 nm) worm-like fibrillary structures were
349 observed both in diluted EW (Figure 6.g and Figure S6) or in diluted EW containing 0.3% (w/v)
350 SDS (Figure 6.h and Figure S6). Low concentrations of SDS may have induced the formation of
351 fibrillary structures in EW but to a lesser extent than noted for OVA. TEM images of diluted EW
352 in 1.0% (w/v) DTT showed mainly amorphous aggregates (Figure S6). In the case of diluted EW
353 containing 0.3% (w/v) SDS and 0.8% (w/v) SDS along with DTT, TEM images indicated the
354 presence of some worm-like fibrillary structures in combination with amorphous aggregates
355 (Figure S6). The SDS induced fibril formation in diluted EW was thus enhanced by DTT.

356 Higher SDS concentrations [$\geq 0.1\%$ (w/v)] in solutions of unheated OVA lead to an increase in
357 ThT fluorescence (Figure 5.b) from *ca.* 4% to *ca.* 20%, suggesting the formation of fibrillary
358 structures. TEM images revealed that large (> 200 nm) intertwined worm-like fibrillary aggregates
359 had been formed (Figure 6.a and Figure S6). OVA protein aggregates were smaller (< 200 nm)
360 when resulting from bringing the protein in 0.3% (w/v) SDS (Figure 6.b and Figure S6) rather than
361 in water. When brought in 0.8% (w/v) SDS, fibrillary aggregates of variable sizes were
362 distinguished (Figure 6.c and Figure S6). Thus, SDS enhances fibrillation in solutions of unheated
363 OVA. Presumably, SDS concentrations below its critical micellar concentration stabilize β -strands
364 in unfolded proteins and thereby promote fibrillation. Micelles formed at high SDS concentrations
365 limit fibril formation or disrupt fibrils already formed⁴⁷⁻⁵⁰. TEM images revealed worm-like
366 fibrillary aggregates of various sizes in solutions of unheated OVA in water and in 0.3% (w/v) or
367 0.8% (w/v) SDS in combination with DTT (Figure S6). Reduction of the single intramolecular

368 disulfide bond in native OVA increases its surface hydrophobicity and may well facilitate protein
 369 fibrillation²⁹. Overall, SDS concentrations up to 0.3% (w/v) either extracted fibrillary structures
 370 from or induced their formation in boiled OVA and EW, whereas SDS concentrations exceeding
 371 0.5% (w/v) also disrupted fibrillary structures. These effects were enhanced when including 1.0%
 372 (w/v) DTT in SDS containing medium.



373
 374 Figure 6. Morphology of fibrils of unheated ovalbumin (OVA) and egg white (EW) or boiled for
 375 15 min OVA (OVA_{100/15min}) and EW (EW_{100/15min}) after isolation/extraction with sodium dodecyl
 376 sulfate (SDS). TEM images of unheated OVA and EW [(a) to (c) and (g) to (i), respectively] or

377 OVA_{100/15min} [(d) to (f)] and EW_{100/15min} [(j) to (l)] isolated/extracted with various concentrations
378 of SDS. Scale bar: 200 nm.

379 CONCLUSIONS

380 Boiling EW leads to formation of AFs. EW fibrils were extracted with three different extraction
381 procedures, suggesting the result is robust and independent of the extraction conditions. AF
382 aggregation of proteins is driven by short aggregation-prone regions (APRs) within the protein
383 sequence that form beta-structured assemblies while the rest of the protein chain decorates these
384 clusters as unfolded polypeptides. In effect this creates a high local concentration of unfolded
385 protein chains that is readily digestible by gastric proteases while only the APRs representing *ca.*
386 10% of the primary sequence remain protected. In comparison most of the proteolytic sites in a
387 folded protein are not or much less accessible.

388 A dense worm-like fibrillary protein network is extracted from boiled EW with 0.01 M HCl
389 from the pellet obtained after treating boiled EW with proteinase K. FTIR spectra, X-ray
390 diffraction patterns and Congo red staining confirm the presence of AFs in this pellet. Treating
391 heated OVA and boiled EW with trypsin extracts both amorphous and fibrillary aggregates while
392 proteinase K mainly extracts amorphous structures. Prior treatment of heated OVA with trypsin
393 allows elegant demonstration by X-ray diffraction and Congo red staining experiments that it
394 contains AFs. Furthermore, SDS enhances the formation of fibrillary structures in both unheated
395 and heated OVA and EW. Concentrations of SDS exceeding 0.5% (w/v) disrupt fibrillary protein
396 structures, an effect which is enhanced in presence of DTT. Our results are the first to show that
397 AFs are present in hard-boiled eggs. The presence of AFs in other food products should be
398 explored. To study the latter, we suggest using an enzymatic extraction protocol as presented in
399 this study. Also, the presence of AFs in hard-boiled egg white questions the role of AFs in the

400 human diet. It would be useful to study the proteolytic resistance of such protein structures in the
401 intestinal tract and to examine their toxicity. Such work will be the topic of a subsequent
402 manuscript. Last but not least, protein functionality can be optimised by exploiting AF formation.
403 Applications thereof include partial or total replacement of animal-based protein by plant proteins
404 in food systems.

405 *Supporting Information Available:* Morphology of (amyloid) protein fibrils in EW_{100/15min} and
406 in unheated, heated and boiled OVA; Impact of peptidases on protein fibril extractability from
407 OVA_{78/22h} and EW_{100/15min} over time; Morphology of protein fibrils extracted with peptidases from
408 OVA_{78/22h} and EW_{100/15min}; Morphology of the components in the SE-HPLC peaks in enzymatic
409 extracts of OVA_{78/22h} and EW_{100/15min}; Morphology of protein fibrils of unheated OVA and EW or
410 OVA_{100/15min} and EW_{100/15min} isolated/extracted with SDS and 1.0% (w/v) DTT.

411 *Acknowledgments.* The authors acknowledge the Research Foundation-Flanders (FWO, SBO
412 grant S003918N Brussels, Belgium). M.A. Lambrecht acknowledges FWO-Flanders for her
413 mandate as postdoctoral researcher (grant 12V6718N). The Switch Laboratory was supported by
414 grants under the EU's Horizon 2020 Framework Programme ERC Grant agreement 647458
415 (MANGO) to J. Schymkowitz, the Flanders Institute for Biotechnology (VIB), the KU Leuven,
416 the FWO-Flanders, the Flanders Agency for Innovation by Science and Technology (IWT, SBO
417 grant 60839) and the Federal Office for Scientific Affairs of Belgium (Belspo), IUAP, grant
418 number P7/16. I. Rombouts and K.J.A. Jansens are gratefully thanked for fruitful discussions. L.
419 Liesenborghs and V. Depoortere are acknowledged for excellent technical assistance. The
420 Laboratory for biocrystallography (KU Leuven) and the Electron Microscopy Platform & Bio
421 Imaging Core (KU Leuven, VIB – KU Leuven Center for Brain & Disease Research) are gratefully
422 thanked for assistance with X-ray diffraction measurements and TEM analysis, respectively. M.

423 Monge-Morera thanks the University of Costa Rica (UCR) for the permission to perform research
424 abroad. J.A. Delcour is W. K. Kellogg Chair in Cereal Science and Nutrition at the KU Leuven
425 and beneficiary of Methusalem excellence funding at the KU Leuven.

426 REFERENCES

- 427 (1) Greenwald, J.; Riek, R. Biology of Amyloid: Structure, Function, and Regulation. *Structure*
428 **2010**, *18*, 1244–1260.
- 429 (2) Serpell, L. Amyloid Structure. *Essays Biochem.* **2014**, *56*, 1–10.
- 430 (3) Knowles, T. P.; Fitzpatrick, A. W.; Meehan, S.; Mott, H. R.; Vendruscolo, M.; Dobson, C.
431 M.; Welland, M. E. Role of Intermolecular Forces in Defining Material Properties of Protein
432 Nanofibrils. *Sci. Reports* **2007**, *318*, 1900–1903.
- 433 (4) Knowles, T. P. J.; Mezzenga, R. Amyloid Fibrils as Building Blocks for Natural and
434 Artificial Functional Materials. *Adv. Mater.* **2016**, *28*, 6546–6561.
- 435 (5) Pearce, F. G.; Mackintosh, S. H.; Gerrard, J. A. Formation of Amyloid-like Fibrils by
436 Ovalbumin and Related Proteins under Conditions Relevant to Food Processing. *J. Agric.*
437 *Food Chem.* **2007**, *55*, 318–322.
- 438 (6) Fowler, D. M.; Koulov, A. V.; Balch, W. E.; Kelly, J. W. Functional Amyloid - from
439 Bacteria to Humans. *Trends Biochem. Sci.* **2007**, *32*, 217–224.
- 440 (7) Knowles, T. P. J.; Buehler, M. J. Nanomechanics of Functional and Pathological Amyloid
441 Materials. *Nat. Nanotechnol.* **2011**, *6*, 469–479.
- 442 (8) Chiti, F.; Dobson, C. M. Protein Misfolding, Amyloid Formation, and Human Disease: A
443 Summary of Progress over the Last Decade. *Annu. Rev. Biochem.* **2017**, *86*, 27–68.
- 444 (9) Rousseau, F.; Schymkowitz, J.; Serrano, L. Protein Aggregation and Amyloidosis:
445 Confusion of the Kinds? *Curr. Opin. Struct. Biol.* **2006**, *16*, 118–126.

- 446 (10) Monsellier, E.; Ramazzotti, M.; Taddei, N.; Chiti, F. Aggregation Propensity of the Human
447 Proteome. *PLoS Comput. Biol.* **2008**, *4*, e1000199.
- 448 (11) Eisenberg, D.; Jucker, M. The Amyloid State of Proteins in Human Diseases. *Cell* **2012**,
449 *186*, 1188–1203.
- 450 (12) Knowles, T. P. J.; Vendruscolo, M.; Dobson, C. M. The Amyloid State and Its Association
451 with Protein Misfolding Diseases. *Nat. Rev. Mol. Cell Biol.* **2014**, *15*, 384–396.
- 452 (13) Jansens, K. J. A.; Lambrecht, M. A.; Rombouts, I.; Monge Morera, M.; Brijs, K.; Rousseau,
453 F.; Schymkowitz, J.; Delcour, J. A. Conditions Governing Food Protein Amyloid Fibril
454 Formation—Part I: Egg and Cereal Proteins. *Compr. Rev. Food Sci. Food Saf.* **2019**, *0*,
455 1256–1276.
- 456 (14) Lambrecht, M. A.; Jansens, K. J. A.; Rombouts, I.; Brijs, K.; Rousseau, F.; Schymkowitz,
457 J.; Delcour, J. A. Conditions Governing Food Protein Amyloid Fibril Formation—Part II:
458 Milk and Legume Proteins. *Compr. Rev. Food Sci. Food Saf.* **2019**, *0*, 1277–1291.
- 459 (15) Solomon, A.; Richey, T.; Murphy, C. L.; Weiss, D. T.; Wall, J. S.; Westermark, G. T.;
460 Westermark, P. Amyloidogenic Potential of Foie Gras. *PNAS* **2007**, *104*, 10998–11001.
- 461 (16) Mine, Y. Recent Advances in Egg Protein Functionality in the Food System. *Worlds. Poult.*
462 *Sci. J.* **2002**, *58*, 31–39.
- 463 (17) Mine, Y.; Noutomi, T.; Hagu, N. Thermally Induced Changes in Egg White Proteins. *J.*
464 *Agric. Food Chem.* **1990**, *38*, 2122–2125.
- 465 (18) Belitz, H.-D.; Grosch, W.; Schierberle, P. Eggs. In *Food Chemistry*; Springer: Berlin,
466 Germany, 2009; pp 546–561.
- 467 (19) Weijers; van de Velde, F.; Stijnman, A.; van de Pijpekamp, A.; Visschers, R. W. Structure
468 and Rheological Properties of Acid-Induced Egg White Protein Gels. *Food Hydrocoll.*

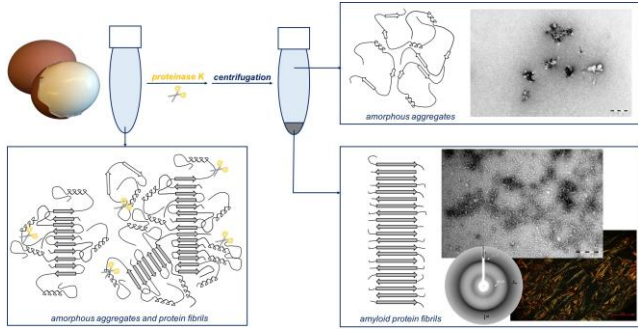
- 469 **2006**, *20*, 146–159.
- 470 (20) Astbury, W. T.; Dickinson, S.; Bailey, K. The X-Ray Interpretation of Denaturation and the
471 Structure of the Seed Globulins. *Biochem. J.* **1935**, *29*, 2351–2360.
- 472 (21) Bhattacharya, M.; Dogra, P. Self-Assembly of Ovalbumin Amyloid Pores: Effects on
473 Membrane Permeabilization, Dipole Potential, and Bilayer Fluidity. *Langmuir* **2015**, *31*,
474 8911–8922.
- 475 (22) Bhattacharya, M.; Jain, N.; Dogra, P.; Samai, S.; Mukhopadhyay, S. Nanoscopic Amyloid
476 Pores Formed via Stepwise Protein Assembly. *J. Phys. Chem. Lett.* **2013**, *4*, 480–485.
- 477 (23) Jansens, K. J. A.; Brijs, K.; Stetefeld, J.; Delcour, J. A.; Scanlon, M. G. Ultrasonic
478 Characterization of Amyloid-like Ovalbumin Aggregation. *ACS Omega* **2017**, *2*, 4612–
479 4620.
- 480 (24) Lara, C.; Gourdin-Bertin, S.; Adamcik, J.; Bolisetty, S.; Mezzenga, R. Self-Assembly of
481 Ovalbumin into Amyloid and Non-Amyloid Fibrils. *Biomacromolecules* **2012**, *13*, 4213–
482 4221.
- 483 (25) Lassé, M.; Ulluwishewa, D.; Healy, J.; Thompson, D.; Miller, A.; Roy, N.; Chitcholtan, K.;
484 Gerrard, J. A. Evaluation of Protease Resistance and Toxicity of Amyloid-like Food Fibrils
485 from Whey, Soy, Kidney Bean, and Egg White. *Food Chem.* **2016**, *192*, 491–498.
- 486 (26) Weijers, M.; Sagis, L. M. C.; Veerman, C.; Sperber, B.; van der Linden, E. Rheology and
487 Structure of Ovalbumin Gels at Low PH and Low Ionic Strength. *Food Hydrocoll.* **2002**,
488 *16*, 269–276.
- 489 (27) Alting, A. C.; Weijers, M.; de Hoog, E. H. A.; van de Pijpekamp, A. M.; Cohen Stuart, M.
490 A.; Hamer, R. J.; de Kruif, C. G.; Visschers, R. W. Acid-Induced Cold Gelation of Globular
491 Proteins: Effects of Protein Aggregate Characteristics and Disulfide Bonding on

- 492 Rheological Properties. *J. Agric. Food Chem.* **2004**, *52*, 623–631.
- 493 (28) Azakami, H.; Mukai, A.; Kato, A. Role of Amyloid Type Cross β -Structure in the Formation
494 of Soluble Aggregate and Gel in Heat-Induced Ovalbumin. *J. Agric. Food Chem.* **2005**, *53*,
495 1254–1257.
- 496 (29) Jansens, K. J. A.; Brijs, K.; Delcour, J. A.; Scanlon, M. G. Amyloid-like Aggregation of
497 Ovalbumin: Effect of Disulfide Reduction and Other Egg White Proteins. *Food Hydrocoll.*
498 **2016**, *61*, 914–922.
- 499 (30) Pouzot, M.; Nicolai, T.; Visschers, R. W.; Weijers, M. X-Ray and Light Scattering Study
500 of the Structure of Large Protein Aggregates at Neutral PH. *Food Hydrocoll.* **2005**, *19*, 231–
501 238.
- 502 (31) Tanaka, N.; Morimoto, Y.; Noguchi, Y.; Tada, T.; Waku, T.; Kunugi, S.; Morii, T.; Lee, Y.
503 F.; Konno, T.; Takahashi, N. The Mechanism of Fibril Formation of a Non-Inhibitory
504 Serpin Ovalbumin Revealed by the Identification of Amyloidogenic Core Regions. *J. Biol.*
505 *Chem.* **2011**, *286*, 5884–5894.
- 506 (32) Weijers, M.; Barneveld, P. A.; Cohen Stuart, M. A.; Visschers, R. W. Heat-Induced
507 Denaturation and Aggregation of Ovalbumin at Neutral PH Described by Irreversible First-
508 Order Kinetics. *Protein Sci.* **2003**, *12*, 2693–2703.
- 509 (33) Weijers, M.; Visschers, R. W. Light Scattering Study of Heat-Induced Aggregation and
510 Gelation of Ovalbumin. *Macromolecules* **2002**, *35*, 4753–4762.
- 511 (34) Numata, K.; Kaplan, D. L. Mechanisms of Enzymatic Degradation of Amyloid Beta
512 Microfibrils Generating Nanofilaments and Nanospheres Related to Cytotoxicity.
513 *Biochemistry* **2010**, *49*, 3254–3260.
- 514 (35) Hartl, F. U.; Bracher, A.; Hayer-Hartl, M. Molecular Chaperones in Protein Folding and

- 515 Proteostasis. *Nature* **2011**, *475*, 324–332.
- 516 (36) Harrison, R. S.; Sharpe, P. C.; Singh, Y.; Fairlie, D. P. Amyloid Peptides and Proteins in
517 Review. In *Review of Physiology Biochemistry and Pharmacology*; Amara, S. G., Bamberg,
518 E., Fleischmann, B., Gudermann, T., Hebert, S. C., Jahn, R., Lederer, W. J., Lilll, R.,
519 Hiyajima, A., Offermanns, S., Zechner, R., Eds.; Springer, Berlin, 2007; Vol. 159, pp 1–77.
- 520 (37) Maurer-Stroh, S.; Debulpaep, M.; Kuemmerer, N.; Lopez de la Paz, M.; Martins, I. C.;
521 Reumers, J.; Morris, K. L.; Copland, A.; Serpell, L. C.; Serrano, L.; Schymkowitz, J. W.
522 H.; Rousseau, F. Exploring the Sequence Determinants of Amyloid Structure Using
523 Position-Specific Scoring Matrices. *Nat. Methods* **2010**, *7*, 237–242.
- 524 (38) Vassar, P. S.; Culling, C. F. Fluorescent Stains, with Special Reference to Amyloid and
525 Connective Tissues. *Arch. Pathol.* **1959**, *68*, 487–498.
- 526 (39) Stsiapura, V. I.; Maskevich, A. A.; Kuzmitsky, V. A.; Uversky, V. N.; Kuznetsova, I. M.;
527 Turoverov, K. K. Thioflavin T as a Molecular Rotor: Fluorescent Properties of Thioflavin
528 T in Solvents with Different Viscosity. *J. Phys. Chem. B* **2008**, *112*, 15893–15902.
- 529 (40) Hackl, E. V.; Darkwah, J.; Smith, G.; Ermolina, I. Effect of Acidic and Basic PH on
530 Thioflavin T Absorbance and Fluorescence. *Eur. Biophys. J.* **2015**, *44*, 249–261.
- 531 (41) Randrianjatovo-Gbalou, I.; Marcato-Romain, C. E.; Girbal-Neuhauser, E. Quantification of
532 Amyloid Fibrils Using Size Exclusion Chromatography Coupled with Online Fluorescence
533 and Ultraviolet Detection. *Anal. Biochem.* **2015**, *488*, 19–21.
- 534 (42) Nichols, M. R.; Moss, M. A.; Reed, D. K.; Lin, W. L.; Mukhopadhyay, R.; Hoh, J. H.;
535 Rosenberry, T. L. Growth of β -Amyloid(1-40) Protofibrils by Monomer Elongation and
536 Lateral Association. Characterization of Distinct Products by Light Scattering and Atomic
537 Force Microscopy. *Biochemistry* **2002**, *41*, 6115–6127.

- 538 (43) Leslie, A. G. W.; Powell, H. R. Processing Diffraction Data with Mosflm. In *Evolving*
539 *Methods for Macromolecular Crystallography*; Read, R. J., Sussman, J. L., Eds.; Springer:
540 Dordrecht, The Netherlands, 2007; Vol. 245, pp 41–51.
- 541 (44) Nilsson, M. R. Techniques to Study Amyloid Fibril Formation in Vitro. *Methods* **2004**, *34*,
542 151–160.
- 543 (45) Sivalingam, V.; Prasanna, N. L.; Sharma, N.; Prasad, A.; Patel, B. K. Wild-Type Hen Egg
544 White Lysozyme Aggregation in Vitro Can Form Self-Seeding Amyloid Conformational
545 Variants. *Biophys. Chem.* **2016**, *219*, 28–37.
- 546 (46) Petkova, A. T.; Leapman, R. D.; Guo, Z.; Yau, W.-M.; Mattson, M. P.; Tycko, R. Self-
547 Propagating, Molecular-Level Polymorphism in Alzheimer’s β -Amyloid Fibrils. *Science*
548 **2005**, *307*, 262–266.
- 549 (47) Pertinhez, T. A.; Bouchard, M.; Smith, R. A. G.; Dobson, C. M.; Smith, L. J. Stimulation
550 and Inhibition of Fibril Formation by a Peptide in the Presence of Different Concentrations
551 of SDS. *FEBS Lett.* **2002**, *529*, 193–197.
- 552 (48) Yamamoto, S.; Hasegawa, K.; Yamaguchi, I.; Tsutsumi, S.; Kardos, J.; Goto, Y.; Gejyo, F.;
553 Naiki, H. Low Concentrations of Sodium Dodecyl Sulfate Induce the Extension of Beta 2-
554 Microglobulin-Related Amyloid Fibrils at a Neutral PH. *Biochemistry* **2004**, *43*, 11075–
555 11082.
- 556 (49) Yagi, H.; Ban, T.; Morigaki, K.; Naiki, H.; Goto, Y. Visualization and Classification of
557 Amyloid Supramolecular Assemblies. *Biochemistry* **2007**, *46*, 15009–15017.
- 558 (50) Rangachari, V.; Reed, D. K.; Moore, B. D.; Rosenberry, T. L. Secondary Structure and
559 Interfacial Aggregation of Amyloid-Beta(1-40) on Sodium Dodecyl Sulfate Micelles.
560 *Biochemistry* **2006**, *45*, 8639–8648.

561 TABLE OF CONTENTS GRAPHIC



562

563

564

565